Autonomous Robots (2023) 47:1245–1254
https://doi.org/10.1007/s10514-023-10124-6

Robust bounded control scheme for quadrotor vehicles under high dynamic disturbances

J. Betancourt[1] · P. Castillo[1] · P. García[2] · V. Balaguer[2] · R. Lozano[1,3]

Received: 18 August 2022 / Accepted: 2 July 2023 / Published online: 21 July 2023

Abstract
In this paper, an optimal bounded robust control algorithm for secure autonomous navigation in quadcopter vehicles is proposed. The controller is developed combining two parts; one dedicated to stabilize the closed-loop system and the second one for dealing and estimating external disturbances as well unknown nonlinearities inherent to the real system's operations. For bounding the energy used by the system during a mission and, without losing its robustness properties, the quadratic problem formulation is used considering the actuators system constraints. The resulting optimal bounded control scheme improves considerably the stability and robustness of the closed-loop system and at the same time bounds the motor control inputs. The controller is validated in real-time flights and in unconventional conditions for high wind-gusts and Loss of Effectiveness in two rotors. The experimental results demonstrate the good performance of the proposed controller in both scenarios.

Keywords Robust bounded control · Quadrotor · Aggressive disturbances · Real-time experiments

1 Introduction

Quadcopters have been the most preferred multi-rotor aerial robot configuration for civilian applications (Aijun and Shamshirband, 2016; Tofigh et al., 2018; Derrouaoui et al., 2022). Due to their simplicity and versatility, quadcopters have attracted the attention of a large part of control and robotic scientific communities in front of other types of UAVs (Shraim et al., 2018). However, quadcopters have some disadvantages; for example, it is an underactuated system, unstable, with nonlinearities and fast dynamics as well as couplings between their different loops. Nevertheless, these disadvantages represent a challenge for the control scientific community (Saeed et al., 2015). One of the main problems for commercial multi-rotors is that their inner control architecture is not conceived for compensating aggressive wind-gust or rotors failures. This problem makes the aerial vehicles not safe for their use on civil applications (or in populated areas). The solutions given in the literature solve only one problem. For example; for dealing with external high disturbances, robust (and/or adaptive) controllers have been proposed (Lopez-Sanchez et al., 2021; Bisheban and Lee, 2021; Fang et al., 2018; Izaguirre-Espinosa et al., 2019), in the case of rotors failures some solutions are given using fault-tolerant control methodologies (Song et al., 2019; Pan et al., 2021; Ban et al., 2020; Ortiz-Torres et al., 2020).

In particular, robustness issues may be critical for quadcopter control since it can be subjected to undesired nonlinear dynamics and external disturbances. In order to weaken the effect of wind gusts, some authors have proposed complex control techniques to achieve stability. In Yang et al. (2020),

✉ J. Betancourt
gjc.betancourt@gmail.com

P. Castillo
castillo@hds.utc.fr

P. García
pggil@isa.upv.es

V. Balaguer
vibagar3@upvnet.upv.es

R. Lozano
rlozano@hds.utc.fr

[1] Heudiasyc (Heuristics and Diagnosis of Complex Systems), CS 60 319 - 60 203, Université de Technologie de Compiègne, 57 Av. de Landshut, 60200 Compiègne, France

[2] Instituto Universitario de Automática e Informática Industrial (AI2), Universitat Politècnica de València (UPV), Camino de Vera S/n, Edificio 8 G Acceso D planta 4, 46022 Valencia, Spain

[3] UMI-LAFMIA, CINVESTAV, Av. IPN 2508, San Pedro Zacatenco 07360, CDMX, Mexico

Jin et al. (2020) and Labbadi and Cherkaoui (2020) adaptive controllers with different structures were proposed and verified by simulations and experiments on test a bench. However, others researchers preferred to apply a Disturbance Observer Based Control (DOBC) strategy for attenuating external/internal disturbances. Among the most used DOBC techniques, it is worth to highlight the followings (Guo and Liang Zhao, 2011; Huang and Xue, 2014; Chen, 2004). In these works, the Disturbance Observer (DOB) uses the transfer function of the system to compare the analytical desired performance with the real one and then, the difference between these inputs of these systems is taken as the disturbance. Despite several works found in the literature that propose guaranteeing robustness of the system, few of them bounds the control inputs for limiting the energy applied in the system. This is because in some cases, bounding the control input only guarantees the robustness in a small range of external disturbances (Chen et al., 2020).

Bounding the control input is a challenge when implementing theoretical control results in real systems. This is due to the fact that, if the control signal exceeds the control inputs limits, it may lead to undesirable behavior of the system and therefore loose the stability. The maneuvering flight of quadrotors may lead to actuator saturation, which commonly affects the flight quality, including trajectory-tracking accuracy. To address actuator saturation during the maneuvering flight of quadrotors, an attitude controller based on the conditioned super-twisting algorithm (CSTA) was designed in Chang et al. (2023). The authors replace the sign function by a hyperbolic tangent function, which suppresses the chattering of the CSTA. In Tripathi et al. (2020) the anti-windup approach was proposed and applied for the autonomous landing problem for UAVs. This anti-windup algorithm was based on the property of convergence for marginally stable linear plants with saturated inputs. Furthermore, in Faessler et al. (2017) an iterative thrust-mixing scheme based on the LQR approach, to compute the desired single rotor thrusts and a prioritizing motor-saturation, was validated in real-time tests. In Smeur et al. (2018), a cascade integration of Incremental Nonlinear Dynamic Inversion (INDI) for the attitude and position control of micro aerial vehicles is addressed. Wind tunnel experiments show that the vehicle can enter and leave the 10 m/s wind tunnel flow with only 21 cm maximum position deviation on average.

In most of all these works, the desired collective thrust and body torques need to be converted into four single rotor thrusts. Consequently, it can be applied by means of the mapping from motors commands to rotor thrusts, i.e., *thrust mapping* (Faessler et al., 2017). For autonomous navigation, aerial vehicles need robust control systems to compensate the adverse effects produced by parametric and non-parametric uncertainties, unknown dynamics and atmospheric disturbances (Azar et al., 2021; Belmouhoub et al., 2022). In flight real-time applications the robot is exposed to these undesired situations, therefore, the controller computes a large amount of energy for counteracting them. Thus, if this energy is sent without a priori knowledge and during large periods of time, the actuators can be overheated and damaged leading to poor performance or undesirable crashes. This situation happens because they have physical constraints that often are not considered when computing the control law, e.g. maximum angular velocity in a motor.

In this work, we propose a simple and efficient robust bounded control algorithm for handling aggressive wind-gust and rotor failures. The control architecture is composed of a disturbance observer and a nominal controller (e.g. controller of a commercial aerial vehicle). Our control design considers the bound of the physical actuators for (1) obtaining optimal bounded control inputs and (2) preventing the saturation of the motors when the system requests extra energy to counteract aggressive disturbances. To the best of our knowledge, this is the first time that disturbances rejection, rotors failures compensation and optimal bounds for actuators are included together in one control algorithm. Our architecture is validated also experimentally in real-time flights under unconventional conditions for high wind-gusts and Loss of Effectiveness (LoE) in two rotors.

The rest of the paper is organized as follows: in Sect. 2, the dynamic model of quadrotor is recalled. The optimal bounded robust control scheme is addressed in Sect. 3. Experimental real-time tests to demonstrate the good performance of the proposed architecture, are provided in Sect. 4. Finally, conclusion and future work are discussed in Sect. 5.

Notation vectors are expressed by bold lower case letters, i.e., $\boldsymbol{v}$, while matrices are represented by bold upper case letters, e.g. $\boldsymbol{R}$. Therefore, scalar letters will be denoted by normal lower case letters.

2 Problem formulation

The dynamic model of a quadcopter can be described by representing the vehicle as a $3D$ rigid body, which is driven by forces and torques generated by the propellers, see Fig 1. Therefore, the nonlinear model of the quadcopter using the Newton–Euler formalism can be expressed as Castillo et al. (2005)

$$\begin{aligned}
&\dot{\boldsymbol{\xi}}(t) = \boldsymbol{v}(t),\\
&m\ddot{\boldsymbol{\xi}}(t) = \boldsymbol{R}(t)\boldsymbol{F}(t) - mg\boldsymbol{e}_z,\\
&\dot{\boldsymbol{R}}(t) = \boldsymbol{R}(t)\hat{\boldsymbol{\Omega}}(t),\\
&\boldsymbol{J}\dot{\boldsymbol{\Omega}} = -\boldsymbol{\Omega}(t) \times \boldsymbol{J}\boldsymbol{\Omega}(t) + \boldsymbol{\tau}(t),
\end{aligned} \tag{1}$$

where $\boldsymbol{\xi}(t)$ denotes the vector position of the vehicle with respect to the inertial frame $\mathscr{I}$, $\boldsymbol{v(t)} \in \mathscr{I}$ describes its

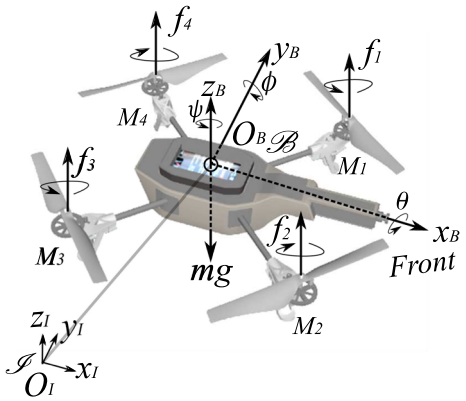

Fig. 1 Quadcopter aerial vehicle representation. $\mathscr{I} = \{x_I, y_I z_I\}$ denotes the inertial frame, and $\mathscr{B} = \{x_B, y_B, z_B\}$ the body frame attached to center of mass of the vehicle. f_i expresses the force applied of motor i

linear velocity, $\boldsymbol{\Omega}(t)$ represents the angular velocity of the body defined in $\mathscr{B}$, and m is its total mass. The constant moment of inertia is $\boldsymbol{J}$ expressed in $\mathscr{B}$, $\boldsymbol{\tau}(t) \triangleq [u_2, u_3, u_4]$ expresses the torques applied in the rigid body, $\hat{\boldsymbol{\Omega}}(t)$ introduces the skew-symmetric matrix of $\boldsymbol{\Omega}(t)$, $\boldsymbol{R}(t)$ means the rotation matrix from the body $\mathscr{B}$ to the inertial $\mathscr{I}$ frames, and $\boldsymbol{F}(t) \triangleq [0, 0, u_1]$ is the force vector applied to the robot.

In this work, it is assumed that the thrust $f_i \approx k_f w_{M_i}^2$, and torque, $\tau_{M_i} \approx k_\tau w_{M_i}^2$, of each propeller are directly controlled by the angular rate of the motor, w_{M_i}, with k_f and k_τ are aerodynamic thrust and torque factors, respectively. Therefore, from (1) and Fig. 1, $\boldsymbol{F}$ and $\boldsymbol{\tau}$ can be written as $\boldsymbol{F} = [0, 0, \sum_{i=1}^{4} f_i]^T$ and $\boldsymbol{\tau} = [l(f_1 + f_4) - l(f_2 + f_3), l(f_1 + f_2) - l(f_3 + f_4), k_\tau(-f_1 + f_2 - f_3 + f_4)]^T$, with l representing the distance from the center of mass to the point where the force is applied.

Thus, the following relation for the control inputs can be established based on the angular rate of the rotors

$$\bar{\mathbf{u}} = \begin{bmatrix} u_1 \\ u_2 \\ u_3 \\ u_4 \end{bmatrix} = \begin{bmatrix} k_f & k_f & k_f & k_f \\ k_f l & -k_f l & -k_f l & k_f l \\ k_f l & k_f l & -k_f l & -k_f l \\ -k_\tau & k_\tau & -k_\tau & k_\tau \end{bmatrix} \begin{bmatrix} \omega_{M_1}^2 \\ \omega_{M_2}^2 \\ \omega_{M_3}^2 \\ \omega_{M_4}^2 \end{bmatrix}. \tag{2}$$

Bounding the controller without degrading the closed-loop system performance is a challenge, and several works have been proposed in the literature (Sun et al., 2017; Cabecinhas et al., 2012; Li et al., 2017; Wang et al., 2021; Gruszka et al., 2013; Konstantopoulos et al., 2016). Nevertheless, most of them only consider the bound in the control laws without taking into account their actuators allocation. In this work, we propose an optimal bounded control algorithm for quadrotor aerial vehicles. The control law is composed by two parts; one dedicated to stabilize the vehicle when it is close to ideal conditions. The second one is capable

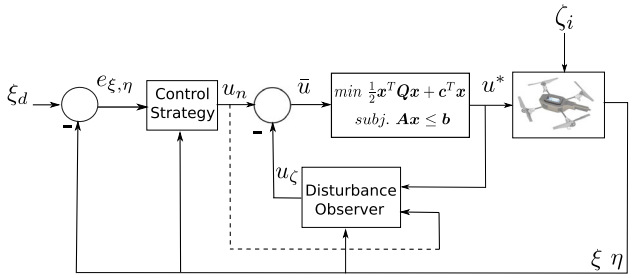

Fig. 2 Block diagram of the control structure. $\mathbf{u}_n$ and $\mathbf{u}_\zeta$ correspond to the nominal control action and the control rejection part, respectively, ξ_d is the desired reference. ξ, η means the position and attitude states. $\bar{u}$ and u^* represent the proposed controller and the set of its optimal and bounded values, respectively. The quadratic problem block deals with the motors constraints and ζ represents external disturbances

of estimating and compensating the endogenous and exogenous properties of the system, such as undesired dynamics (produced by fault in motors) or external perturbations. In addition, the controller is developed to find the optimal values of the control law to avoid saturation or overheat the actuators. The proposed optimal bounded robust control architecture is depicted in Fig. 2.

3 Optimal bounded robust control scheme

System (1) can be also expressed as a perturbed nonlinear system with the form

$$\dot{\mathbf{x}}(t) = \mathbf{A}\mathbf{x}(t) + \mathbf{B}\bar{\mathbf{u}}(t) + \mathbf{f}(\mathbf{x}, \bar{\mathbf{u}}, t) + \mathbf{d}(t) \tag{3}$$

where $\mathbf{A} \in \mathbb{R}^{nxn}$ and $\mathbf{B} \in \mathbb{R}^{nxm}$ are the system matrices, $\mathbf{x}(t) = [\boldsymbol{\xi}, \boldsymbol{\eta}]^T \in \mathbb{R}^n$ and $\bar{\mathbf{u}}(t) \in \mathbb{R}^m$ are the state and control vectors respectively, $\mathbf{f}(\mathbf{x}, \bar{\mathbf{u}}, t) : \mathbb{R}^n \times \mathbb{R} \times \mathbb{R}^+ \to \mathbb{R}^n$ defines an unknown non-linear function, and $\mathbf{d}(t) : \mathbb{R}^+ \to \mathbb{R}^n$ denotes the vector of unknown external disturbances. $\boldsymbol{\eta}$ represents the attitude vector of the vehicle, with $\Omega = \mathbf{W}_\eta \dot{\eta}$ and $\mathbf{W}_\eta$ defines the standard kinematics relation between Ω and $\boldsymbol{\eta}$. The full state is assumed to be measurable. The equations of the model (1) can be written in the form of (3) as Bouabdallah et al. (2004):

$$\mathbf{A} = \begin{bmatrix} 0_6 & I_6 \\ 0_6 & 0_6 \end{bmatrix}, \ \mathbf{B} = \begin{bmatrix} 0_6 \\ \bar{\mathbf{B}} \end{bmatrix}, \mathbf{f} = \begin{bmatrix} 0_6 \\ \bar{\mathbf{f}} \end{bmatrix}, \ \mathbf{d} = \begin{bmatrix} 0_6 \\ \bar{\mathbf{d}} \end{bmatrix}$$

where $\bar{\mathbf{d}} = [\mathbf{d}_\xi, \mathbf{d}_\eta]^T$, $\bar{\mathbf{B}} = [m^{-1}, m^{-1}, (m^{-1} - g), I_x^{-1}, I_y^{-1}, I_z^{-1}]^T$ and $\bar{\mathbf{f}}$ is composed by $\bar{f}_1 = \frac{\cos\phi \sin\theta \cos\psi + \sin\phi \sin\psi}{m} u_1$, $\bar{f}_2 = \frac{\cos\phi \sin\theta \sin\psi - \sin\phi \cos\psi}{m} u_1$, $\bar{f}_3 = \frac{u_1}{m}(1 - \cos\phi \cos\theta)$, $\bar{f}_4 = \frac{(I_y - I_z)}{I_x}\dot{\theta}\dot{\psi} - \frac{J}{I_x}\dot{\theta}\Omega$, $\bar{f}_5 = \frac{(I_z - I_x)}{I_y}\dot{\psi}\dot{\phi} + \frac{J}{I_y}\dot{\phi}\Omega$ and $\bar{f}_6 = \frac{(I_x - I_y)}{I_z}\dot{\theta}\dot{\phi}$.

Assumption 1 The nonlinear function $\frac{\partial[\mathbf{f}(x,\bar{u}) + \mathbf{B}\bar{u}]}{\partial \bar{u}} \neq 0$, for all $(\mathbf{x}, \bar{\mathbf{u}}) \in \mathbb{R}^n \times \mathbb{R}^m$.

Assumption 2 The lumped disturbance $\mathbf{f}(x, \bar{u}) + \mathbf{d}(t)$ is bounded as well as its derivative.

3.1 Control law

The goal is to regulate the state $x(t)$ of the closed-loop system so that it asymptotically tracks the state of the reference model

$$\dot{\mathbf{x}}_q(t) = \mathbf{A}_q \mathbf{x}_q(t) + \mathbf{B}_q r_q(t), \tag{4}$$

where $\mathbf{x}_q \in \mathbb{R}^n$, $\mathbf{A}_q \in \mathbb{R}^{n\times n}$ and $\mathbf{B}_q \in \mathbb{R}^{n\times m}$ are the state vector, the state matrix and the control vector, respectively and A_q a Hurwitz matrix.

The goal is that $\mathbf{x} \to \mathbf{x}_q$, therefore, the following error can be proposed

$$\mathbf{e} = (\boldsymbol{\xi} - \boldsymbol{\xi}_q, \boldsymbol{\eta} - \boldsymbol{\eta}_q)^\top = \mathbf{x} - \mathbf{x}_q. \tag{5}$$

Differentiating (5) and using (3), (4) such that adding and subtracting $\mathbf{A}_q\mathbf{x}$ it holds that

$$\dot{\mathbf{e}} = \mathbf{A}_q\mathbf{e} - \Gamma, \tag{6}$$

with

$$\Gamma = \mathbf{A}\mathbf{x} - \mathbf{A}_q\mathbf{x} - \mathbf{B}_q r_q + \mathbf{B}\bar{\mathbf{u}} + \mathbf{f}(\mathbf{x}, \bar{\mathbf{u}}, t) + \mathbf{d}(t)$$

Observe that if $\Gamma \to 0$ then (6) will be asymptotically stable. Hence, $\bar{\mathbf{u}}$ can be proposed as

$$\bar{\mathbf{u}} = \mathbf{B}^+ \left[\overbrace{\left[(\mathbf{A}_q - \mathbf{A})\mathbf{x} + \mathbf{B}_q r_q\right]}^{\mathbf{u}_n} - \underbrace{[\mathbf{f}(\mathbf{x}, \bar{\mathbf{u}}, t) + \mathbf{d}(t)]}_{\mathbf{u}_\zeta} \right] \tag{7}$$

where $\mathbf{B}^+ = (\mathbf{B}^T\mathbf{B})^{-1}\mathbf{B}^T$ corresponds to the pseudo-inverse of $\mathbf{B}$. The first part of the proposed control law concerns to the reference tracking performance of the linear system (4). On the other hand, $\mathbf{u}_\zeta$ will contain the non-linear part of the controller. Then, the goal will be to compute $\mathbf{u}_n$ and u_ζ. $\mathbf{u}_n = \mathbf{K}\mathbf{x}(t) + \mathbf{B}^+\mathbf{B}_q\mathbf{r}_q(t)$, with $\mathbf{K} = \mathbf{B}^+(\mathbf{A}_q - \mathbf{A})$ representing the control part for stabilizing the system in ideal conditions.

In addition, observe that $\mathbf{u}_\zeta$ is a function of unknown variables, i.e., $\mathbf{u}_\zeta = \mathbf{f}(\mathbf{x}, \bar{\mathbf{u}}, t) + \mathbf{d}(t)$, and therefore it is difficult to estimate this parameter in this form. However, using (3), it can be rewritten as

$$\mathbf{u}_\zeta = \mathbf{B}^+[\mathbf{A}\mathbf{x} + \mathbf{B}\bar{\mathbf{u}} - \dot{\mathbf{x}}]. \tag{8}$$

From (8), we can deduce that the unknown dynamics and disturbances can be estimated from the known dynamics of the systems and control signal. Computing $\mathbf{u}_\zeta$ in the form (8) is not causal but $\mathbf{u}_\zeta$ will be implemented in a micro-controller. Hence for solving it, the Laplace transform is applied. Then, (8) becomes

$$\mathbf{u}_\zeta(s) = \mathbf{G}_f(s)\mathbf{B}^+[\mathbf{A}\mathbf{x}(s) + \mathbf{B}\bar{\mathbf{u}}(s) - s\mathbf{x}(s)]. \tag{9}$$

Assume $\mathbf{G}_f(s)$ is a strictly proper stable low-pass filter with unity gain and zero pahse shift over the spectrum of the uncertain term $\mathbf{f}(\mathbf{x}, \bar{\mathbf{u}}, t) + \mathbf{d}(t)$. From Assumption 2, the asymptotic stability of the closed-loop system for multi-rotor vehicles can be demonstrated as in Zhong and Rees (2004).

3.2 Bounded observer

In quadrotor systems the real control inputs are related with the energy computed by the motors using the relation of the control inputs $\bar{\mathbf{u}}$, as can be stated in (2), for obtaining the angular velocities of each motor. This relation is often obtained when the control laws $\bar{\mathbf{u}}$ need to be transformed into the real control inputs, i.e., the actuators (motors). For the quadrotor vehicle it can be expressed as

$$\mathbf{M} = \mathbf{H}\bar{\mathbf{u}}, \tag{10}$$

with

$$\mathbf{M} = \begin{bmatrix} M_1(t) \\ M_2(t) \\ M_3(t) \\ M_4(t) \end{bmatrix}; \qquad \bar{\mathbf{u}} = \begin{bmatrix} u_1(t) \\ u_2(t) \\ u_3(t) \\ u_4(t) \end{bmatrix} = \begin{bmatrix} u_{n_1} + u_{\zeta_1} \\ u_{n_2} + u_{\zeta_2} \\ u_{n_3} + u_{\zeta_3} \\ u_{n_4} + u_{\zeta_4} \end{bmatrix};$$

and $\mathbf{H}$ denotes the allocation control matrix with the form

$$\mathbf{H} = \begin{bmatrix} 1 & 1 & 1 & -1 \\ 1 & -1 & 1 & 1 \\ 1 & -1 & -1 & -1 \\ 1 & 1 & -1 & 1 \end{bmatrix}$$

Notice that (10) represents the real robust control input applied to the ith actuator (M_i) for controlling the aerial vehicle. If the vehicle is affected by external disturbances or undesired dynamics, the controller needs to be able to estimate and compensate them. However, when the quadrotor is dealing with aggressive and constant perturbations or repetitive missions (tests), the motors can be overheated in several cases, resulting in a physical damage or degradation on its performance. For avoiding that, it is necessary to compute a set of the optimal bounded control inputs, $\mathbf{u}^*$, from $\bar{\mathbf{u}}$.

Hence, $\mathbf{u}^*$ can be obtained as

$$\mathbf{u}^* = \boldsymbol{\delta_M}^T\bar{\mathbf{u}}, \tag{11}$$

where $\boldsymbol{\delta_M}^T = [\delta_1\ \delta_2\ \delta_3\ \delta_4]$ with δ_i defining a factor for fulfilling the rotors constraints. The bounds for the motors control inputs can be found solving the following quadratic problem

$$\min_{\boldsymbol{\delta_M}} \ \frac{1}{2}\boldsymbol{\delta_M}^T\mathbf{Q}\boldsymbol{\delta_M} + \mathbf{c}^T\boldsymbol{\delta_M} \tag{12}$$

$$st.\ \mathbf{A}_M\boldsymbol{\delta_M} \leq \mathbf{b}, \tag{13}$$

where $\mathbf{Q} \in \mathbb{R}^{n\times n}$ is symmetric, $\mathbf{c} \in \mathbb{R}^n$, $\mathbf{A}_M \in \mathbb{R}^{p\times n}$, $\mathbf{b} \in \mathbb{R}^p$ are matrices and vectors that define the optimization problem (Nocedal and Wright, 2006). These parameters are obtained for finding the minimum of the quadratic problem with a cost-to-go function defined as

$$f_o = \sum_{i=1}^{4} Q_i(\bar{u}_i - u_i^*)^2, \tag{14}$$

where Q_i is a weight value penalizing the control input. Developing the above equation, it follows that

$$f_o = \sum_{i=1}^{4} Q_i(\bar{u}_i^2 - 2\delta_i\bar{u}_i^2 + \delta_i^2\bar{u}_i^2). \tag{15}$$

From (15), note that the first term $\bar{u}_i^2$ in parentheses does not affect the computation of the minimum of the quadratic problem, thus, it can be neglected. Developing (15) for $i = 1:4$ and rewriting them in matrix form, it yields

$$f_o = \frac{1}{2}\boldsymbol{\delta_M}^T\mathbf{Q}\boldsymbol{\delta_M} + \mathbf{c}^T\boldsymbol{\delta_M},$$

with

$$\mathbf{Q} = \begin{bmatrix} Q_1\bar{u}_1^2 & 0 & 0 & 0 \\ 0 & Q_2\bar{u}_2^2 & 0 & 0 \\ 0 & 0 & Q_3\bar{u}_3^2 & 0 \\ 0 & 0 & 0 & Q_4\bar{u}_4^2 \end{bmatrix}, \qquad \boldsymbol{c} = \begin{bmatrix} -Q_1\bar{u}_1^2 \\ -Q_2\bar{u}_2^2 \\ -Q_3\bar{u}_3^2 \\ -Q_4\bar{u}_4^2 \end{bmatrix}.$$

let us introduce the constraints on the motors control inputs with the form $\underline{\sigma}_i \leq M_i \leq \bar{\sigma}_i$, where $\bar{\sigma}_i$ and $\underline{\sigma}_i$ are the upper and lower bounds of the motors, respectively. Moreover, define u_0^* as the equilibrium point of the aerial robot at hover position, in other words, the u_1 needed to compensate the weight of the vehicle.

For finding condition (13), consider the case of the motor $M_1 \leq |\sigma_1|$. Thus, taking into account the weight compensation u_0^* and using (10) with the optimal value of $\bar{\mathbf{u}}$ (11), it follows that

$$|\delta_1|\,|\bar{u}_1| + |\delta_2|\,|\bar{u}_2| + |\delta_3|\,|\bar{u}_3| - |\delta_4|\,|\bar{u}_4| \leq |\sigma_1| - u_0^*. \tag{16}$$

Rewriting the previous equation in a general form, it follows that

$$\left|\sum_{i=1}^{4} \pm\delta_i \bar{u}_i\right| \leq |\bar{\sigma}_i| - u_0^*. \tag{17}$$

Therefore, using (17) for all the motors ($i \in [1, 4]$), it is possible to find the values of Eq. (13) as

$$\mathbf{A}_M = \begin{bmatrix} +\bar{u}_1 & +\bar{u}_2 & +\bar{u}_3 & -\bar{u}_4 \\ +\bar{u}_1 & -\bar{u}_2 & +\bar{u}_3 & +\bar{u}_4 \\ +\bar{u}_1 & -\bar{u}_2 & -\bar{u}_3 & -\bar{u}_4 \\ +\bar{u}_1 & +\bar{u}_2 & -\bar{u}_3 & +\bar{u}_4 \\ -\bar{u}_1 & -\bar{u}_2 & -\bar{u}_3 & +\bar{u}_4 \\ -\bar{u}_1 & +\bar{u}_2 & -\bar{u}_3 & -\bar{u}_4 \\ -\bar{u}_1 & +\bar{u}_2 & +\bar{u}_3 & +\bar{u}_4 \\ -\bar{u}_1 & -\bar{u}_2 & +\bar{u}_3 & -\bar{u}_4 \end{bmatrix}, \mathbf{b} = \begin{bmatrix} \bar{\sigma}_1 - u_0^* \\ \bar{\sigma}_2 - u_0^* \\ \bar{\sigma}_3 - u_0^* \\ \bar{\sigma}_4 - u_0^* \\ -\underline{\sigma}_1 + u_0^* \\ -\underline{\sigma}_2 + u_0^* \\ -\underline{\sigma}_3 + u_0^* \\ -\underline{\sigma}_4 + u_0^* \end{bmatrix}.$$

Notice that with the previous equations it is possible to obtain the optimal bounded values $\mathbf{u}^*$ by solving the optimization problem (12) with constraints (13).

Once obtained these values in $\mathbf{u}^*$, the disturbance observer (9) can be rewritten in terms of the optimal inputs (11) as

$$\mathbf{u}_\xi(s) = \mathbf{G}_f(s)\mathbf{B}^+[\mathbf{A}\mathbf{x}(s) + \mathbf{B}\mathbf{u}^*(s) - s\mathbf{x}(s)] \tag{18}$$

with $G_f(s) = \frac{1}{T_f s+1}$, and $T_f > T$, being T the sample-time. The asymptotic stability of the closed-loop system for multi-rotor vehicles can be demonstrated as in Sanz et al. (2017).

4 Experimental results

The practical goal of these experiments is to validate the proposed control architecture. To better illustrate the good performance of the optimal bounded robust controller (11), it is compared, in two scenarios, with respect to its nominal form (7). It is worth to mention that both algorithms have a low computational cost, which permits to be implemented in low cost CPU. The experimental tests are performed in a quadcopter vehicle AR Drone 2. Its firmware was modified to work under the software Fl-AIR - free Framework AIR which is open source and runs a Linux-based operating system, capable of implementing a wide range of control schemes, see Lab (2012). An OptiTrack motion capture system was used to estimate the vehicle's position, while its internal Inertial Measurement Unit (IMU) measures its orientation and angular rates. A video of the experimental results can be seen in https://youtu.be/El7xDcuCas8

The control parameters are presented in the Table 1. Here, $\bar{K}_{1_i}$, $\bar{K}_{2_i}$, express the gains of the controller $\mathbf{u}_n$ for each subsystem, i : $\phi, \theta, \psi, x, y, z$. Each state in (4) can be considered decoupled and modeled by a double integrator with the form $G(s) = b/s^2$ such that b can obtained experimentally for each state. For control implementation the following low-pass filter $G_f = 1/(Ts + 1)$ is used, with T_f representing its bandwidth. The *Eiquadprog* library (LAAS-CNRS, 2009), which uses the algorithm of Goldfarb and Idnani, was implemented for the solution of the convex quadratic problem (12) with constraints (13).

The control gains $\bar{K}_{1_i}$ and $\bar{K}_{2_i}$ of the nominal controller $\mathbf{u}_n$ were tuned in the following way; first, the yaw control gains are tuned and once this dynamics is stabilized, the pitch (or roll) dynamics is tuned as well. The next step is to tune the control gains of the altitude and later the longitudinal (or lateral) dynamics. In each subsystem, the velocity (angular or translational) needs to be tuned first. The observer parameter b_i was obtained experimentally using the Pseudo Random Binary Sequence (PRBS) method while the parameter T_f was also tuned experimentally using the condition $0 < T_f < 1$.

Table 1 Gain parameters used in the experimental tests

Parameter	ϕ, θ	ψ	x, y	z
$\bar{K}_{1_i}$	0.8	0.6	0.17	0.3
$\bar{K}_{2_i}$	0.1	0.2	0.13	0.1
b	140	44	10	5
T_f	0.1	0.5	0.5	0.3

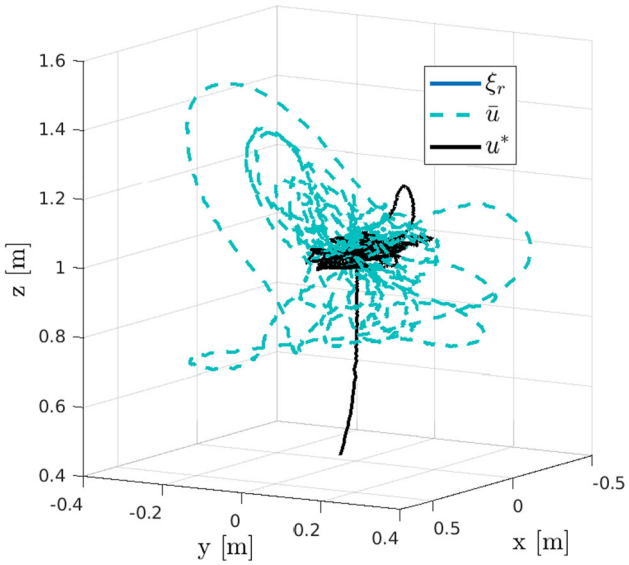

Fig. 3 Scenario 1: Quadrotor position performance when using the UDE-based conntroller and the proposed architecture $\mathbf{u}^*$. Notice that when using the UDE-based conntroller $\bar{\mathbf{u}}$, the performance is degraded and thus the error increases. This error is smaller when using the robust bounded controller $\mathbf{u}^*$

4.1 First scenario: Aggressive wind-gust

Most of the aerial robot applications are developed in outdoors environments where robustness with respect to wind is a primary task. The goal of the first scenario is to show the performance of the quadcopter while it is at hover, subject to aggressive constant and intermittent wind-gust.

Our experiment is considered aggressive as a result of exposing the quadrotor to wind gusts with an airflow speed of 60 km/h and placed at 1.5m of the source of this wind. Some works in the literature present experimental results with wind disturbances generated with nozzle or fans (or similar) generating up to 6m/s of environmental wind, see for example (Byun et al., 2020; Alexis et al., 2010; Waslander and Wang, 2009). The tool used for emulating the wind gusts in our experiment is a leaf blower *Bosch AVS1*. The wind used in this work consists of two main components, a static dominant wind direction and strength, and a wind gust model dependent on a standard power spectral density. In the experiment the quadrotor is at hover position ($x(0) = 0$, $y(0) = 0$, $z(0) = 1$ all in meters) and the wind-gusts are applied for perturbing the aerial vehicle in different directions. A video of the experimental results can be seen in https://youtu.be/0SrcbkVlmUg.

In Fig. 3 the performance of the vehicle in 3D space subject to high wind-gust is introduced. Notice the better performance of the optimal bounded robust controller $\mathbf{u}^*$ with respect to $\bar{\mathbf{u}}$. The position behavior of the drone is depicted in Fig. 4. In the experiment the wind-gust was directed to the y-axis the firsts 20s. Note that both approaches suffer a degradation in their performance, nevertheless it is clear that when using $\mathbf{u}^*$, this degradation (specially in z) is smoother.

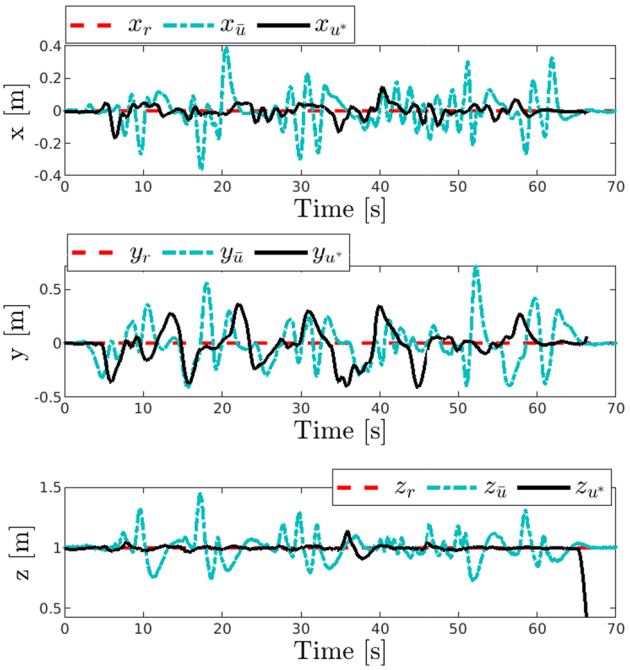

Fig. 4 Scenario 1: System performance during flight tests

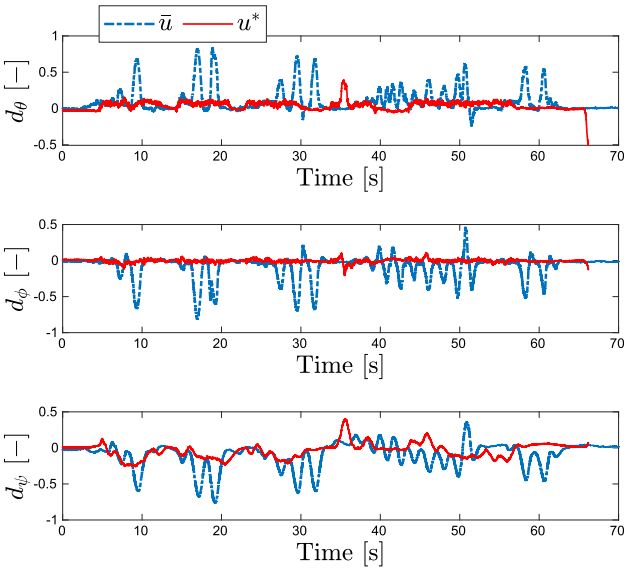

Fig. 5 Scenario 1: Estimation of the wind disturbance on the attitude system. Observe that without the optimal control input, the estimation of the perturbations are bigger producing more instability into the system

Figures 5 and 6 depicts the performance of the disturbance estimations and the motors control input. Notice the relation between these figures. When the disturbance estimation is computed in the controller for compensating these undesired dynamics, notice that the nominal controller $\bar{\mathbf{u}}$, computes higher values exceeding the limits constraints in actuators (in our case is 1). However, when the vehicle is controlled by $\mathbf{u}^*$, observe that the aforementioned problem does not appear.

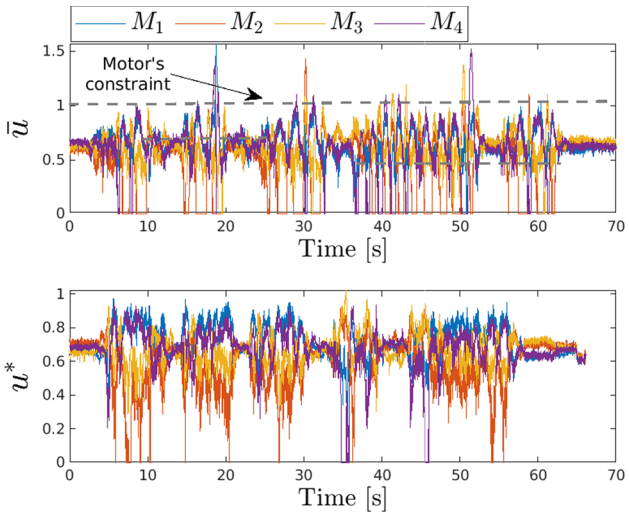

Fig. 6 Scenario 1: Rotors control action's performances, when aggressive wind-gust is applied during a hover position. Notice that if the optimal control is not solved, the input applied to motors of the vehicle will exceed the security limit, 1 in our case, that can produce their saturation and/or damage of the actuators. However, when using our proposed solution, this constraint is never reached guaranteeing that the actuators will not be damaged

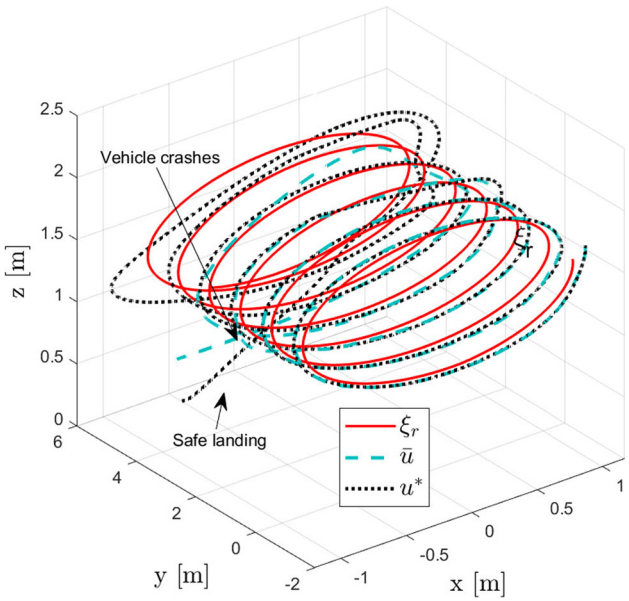

Fig. 7 Scenario 2: 3D state performances in flight tests

4.2 Second scenario: Loss of effectiveness in rotors when performing a trajectory

conducting electrical inspections with drones has been an application developed through the last years. In this kind of tasks, the vehicle needs to be robust with respect to many factors, as wind-gust, possible loss of effectiveness in rotors (repetitive tasks), among others.

The goal of the second scenario is to show the performance of the quadcopter when two LoE in motors M_1 and M_2 occur while performing a desired trajectory emulating conduct electrical inspection. In this experiment, the efficiency in M_1 is reduced 40% at time $t \sim 28$s and,

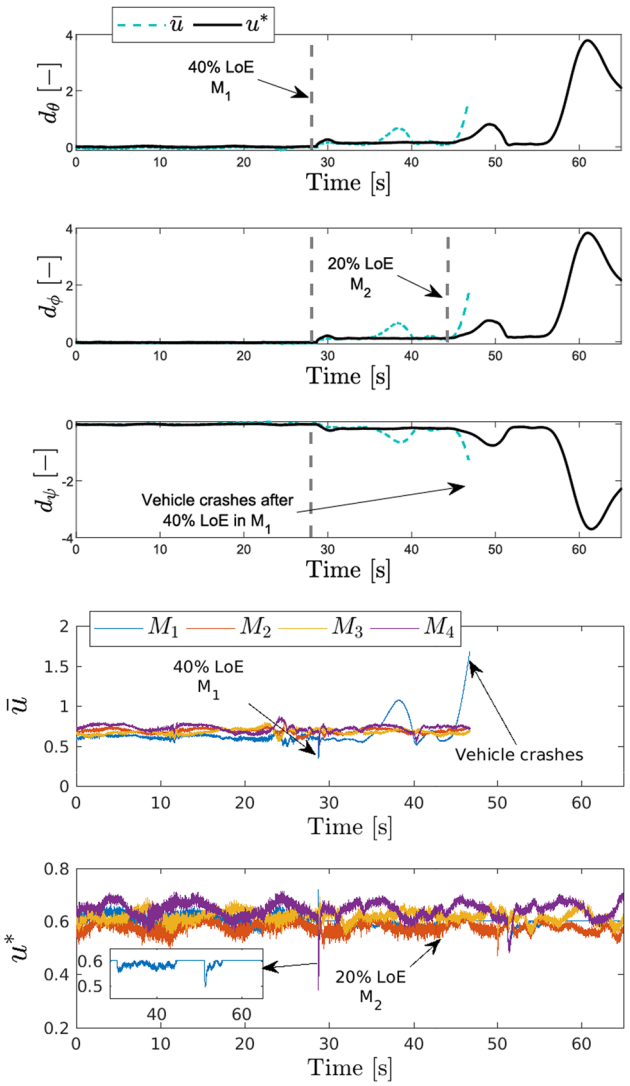

Fig. 8 Scenario 2: Attitude disturbance estimation and motor control action performances

later, at time $t \sim 44$s, the efficiency in M_2 is reduced 20%. A helical trajectory with the form $x_r(t) = t$, $y_r(t) = a\sin(t)$ and $z_r(t) = a\cos(t)$ was chosen as desired trajectory, where a indicating the radius of the circumference. The initial conditions are defined as $\xi_r(0) = [-1,\ 1,\ 2]^T$ in meters. A video of this experiment can be seen at https://youtu.be/rp0u8eeerh0.

Figures 7 and 8 show the performance of the quadcopter, while tracking the helical trajectory subject to LoE in two rotors. The behavior of the vehicle in 3D space is presented in Fig. 7. Notice from this figure that when the first LoE (40%) in rotor M_1 was injected, the practical stability, when using $\bar{\mathbf{u}}$, is compromised perturbing the drone. Moreover, this controller was not capable of guaranteeing stability of the system and therefore, it was not possible to apply the second LoE in rotor M_2 because the aerial robot crashed. Nevertheless, when using $\mathbf{u}^*$, the quadcopter can continue tracking the desired reference and even though, compensate a second LoE (20%) in rotor M_2 at time $t \sim 44$ s.

Figure 8 introduces the behavior of the disturbance estimation and the motor control inputs. Observe from these figures that when using $\mathbf{u}^*$, the vehicle suffers a small degradation on their performance without exceeding the physical constraints of the motors and even though, it can overcome the second LoE around $t \sim 44$s allowing to continue tracking the desired reference and landing safely.

5 Conclusions

An optimal bounded robust control algorithm was developed in this paper. This controller was conceived to be robust with respect to uncertain dynamics and external and unknown perturbations. Its structure contains two parts, one for stabilizing the aerial vehicle close to the ideal conditions (small angles) and the second one for estimating and compensating unknown dynamics. For improving robustness and avoid saturating the actuators of the system, the obtained controller of this scheme was bounded solving a quadratic problem in the control inputs and taking into account the motors constraints.

The proposed architecture was proved, in practice, when several wind-gust were applied while the vehicle was at hover. In addition, the scheme was also validated when loss of effectiveness (LoE) in rotors appears. Here, the practical goal was to track a desired trajectory while two LoE (one of 40% and the second of 20%) in two different motors were applied. Practical validations demonstrated the good performance of the proposed optimal bounded robust controller. Future work includes the analysis of the bounded stability region of the overall system. This implies that the bounds of the lumped term of the Eq. (3) should be addressed. In addition, the analysis of the term T_f and its variation w.r.t. time of the closed loop system will be explored for aerial transportation of suspended payload applications. Finally, the practical stability of the proposed approach when total rotor faults occurs will be investigated.

Supplementary Information The online version contains supplementary material available at https://doi.org/10.1007/s10514-023-10124-6.

Acknowledgements This work was supported by CONACyT (Consejo Nacional de Ciencia y Tecnologiía), Mexico. This work has been also sponsored by the French government research programm Robotex Equipment of Excellence (ANR-10-EQPX-44), the Spanish Ministry of Science, Innovation and Universities, Programme "Estancias de profesores e investigadores senior en centros extranjeros, incluido el Programa Salvador de Madariaga 2019, PRX19/00411" and the scholarships for mobility 2019, "FPI-UPV project PAID-01-17", Universitat Politècnica de València (Spain). The supports are gratefully acknowledged.

Author Contributions All authors contributed equally to this work.

Funding The funding was provided by the CONACyT- Mexico and the program Robotex Equipment of Excellence (ANR-10-EQPX-44).

Declaration

Conflict of interest The authors declare that they have no conflict of interest.

References

Aijun, L., & Shamshirband, S. (2016). A review of quadrotor UAV: Control methodologies and performance evaluation. *International Journal of Automation and Control, 10*(2), 87–103.

Alexis, K., Nikolakopoulos, G., & Tzes, A. (2010). Experimental model predictive attitude tracking control of a quadrotor helicopter subject to wind-gusts. In *18th mediterranean conference on control and automation, med'10* (pp. 1461–1466).

Azar, A., Serrano, F., Koubaa, A., Ibrahim, H., Ahmad Kamal, N., Khamis, A., & Precup, R.-E. (2021). Robust fractional order sliding mode control design for UAVs subjected to atmospheric disturbances (pp. 103–128).

Ban, W., Yanyan, S., & Youmin, Z. (2020). Active fault-tolerant control for a quadrotor helicopter against actuator faults and model uncertainties. *Aerospace Science and Technology, 99*, 105745.

Belmouhoub, A., Medjmadj, S., Bouzid, Y., Derrouaoui, S. H., & Guiatni, M. (2022). Enhanced backstepping control for an unconventional quadrotor under external disturbances. *Aeronautical Journal, 107343*, 1–24.

Bisheban, M., & Lee, T. (2021). Geometric adaptive control with neural networks for a quadrotor in wind fields. *IEEE Transactions on Control Systems Technology, 29*(4), 1533–1548.

Bouabdallah, S., Noth, A., Siegwart, R., & Siegwan, R. (2004). PID versus LQ control techniques applied to an indoor micro quadrotor. In *2004 IEEE/RSJ international conference on intelligent robots and systems (IROS) (IEEE Cat. No.04CH37566)* (Vol. 3, pp. 2451–2456).

Byun, J., Mäkiharju, S. A., & Mueller, M. W. (2020). A flow disturbance estimation and rejection strategy for multirotors with round-trip trajectories. *International Conference on Unmanned Aircraft Systems (ICUAS), 2021*, 1314–1320.

Cabecinhas, D., Cunha, R., & Silvestre, C. (2012). Saturated output feedback control of a quadrotor aircraft. *American Control Conference (ACC), 2012*, 4667–4602.

Castillo, P., Lozano, R., & Dzul López, A. E. (2005). *Modelling and control of mini-flying machines*. London: Springer.

Chang, Z., Chu, H., & Shao, Y. (2023). Quadrotor trajectory-tracking control with actuator saturation. *Electronics, 12*(3), 484.

Chen, J., Wang, J., & Wang, W. (2020). Robust adaptive control for nonlinear aircraft system with uncertainties. *Applied Sciences, 10*(12), 4270.

Chen, W.-H. (2004). Disturbance observer based control for nonlinear systems. *IEEE/ASME Transactions on Mechatronics, 9*(4), 706–710.

Derrouaoui, S. H., Bouzid, Y., Guiatni, M., & Dib, I. (2022). A comprehensive review on reconfigurable drones: Classification, characteristics, design and control technologies. *Unmanned Systems, 10*(01), 3–29.

Faessler, M., Falanga, D., & Scaramuzza, D. (2017). Thrust mixing, saturation, and body-rate control for accurate aggressive quadrotor flight. *IEEE Robotics and Automation Letters, 2*(2), 476–482.

Fang, X., Liu, F., & Ding, Z. (2018). Robust control of unmanned helicopters with high-order mismatched disturbances via disturbance-compensation-gain construction approach. *Journal of the Franklin Institute, 355*(15), 7158–7177.

Gruszka, A., Malisoff, M., & Mazenc, F. (2013). Bounded tracking controllers and robustness analysis for UAVs. *IEEE Transactions on Automatic Control, 58*(1), 180–187.

Guo, B.-Z., & Liang Zhao, Z. (2011). On the convergence of an extended state observer for nonlinear systems with uncertainty. *Systems & Control Letters, 60*(6), 420–430.

Huang, Y., & Xue, W. (2014). Active disturbance rejection control: Methodology and theoretical analysis. *ISA Transactions, 53*(4), 963–976. Disturbance Estimation and Mitigation.

Izaguirre-Espinosa, C., Muñoz-Vazquez, A. J., Sanchez-Orta, A., Parra-Vega, V., & Fantoni, I. (2019). Fractional-order control for robust position/yaw tracking of quadrotors with experiments. *IEEE Transactions on Control Systems Technology, 27*(4), 1645–1650.

Jin, X.-Z., He, T., Wu, X.-M., Wang, H., & Chi, J. (2020). Robust adaptive neural network based compensation control of a class of quadrotor aircrafts. *Journal of the Franklin Institute, 357*(17), 12241–12263.

Konstantopoulos, G. C., Zhong, Q.-C., Ren, B., & Krstic, M. (2016). Bounded integral control of input-to-state practically stable nonlinear systems to guarantee closed-loop stability. *IEEE Transactions on Automatic Control, 61*(12), 4196–4202.

LAAS-CNRS, & Gabriele Buondonno. (2009). Eiquadprog. https://gitlab.laas.fr/stack-oftasks/eiquadprog, Sidst set 12/09/2022.

Lab, H. (2012). Flair—framework libre air. https://devel.hds.utc.fr/software/flair, Sidst set 27/06/2021.

Labbadi, M., & Cherkaoui, M. (2020). Robust adaptive nonsingular fast terminal sliding mode tracking control for an uncertain quadrotor UAV subjected to disturbances. *ISA Transactions, 99*, 290–304.

Li, S., Wang, Y., & Tan, J. (2017). Adaptive and robust control of quadrotor aircrafts with input saturation. *Nonlinear Dynamics, 89*, 255–265.

Lopez-Sanchez, I., Rossomando, F., Pérez- Alcocer, R., Soria, C., Carelli, R., & Moreno-Valenzuela, J. (2021). Adaptive trajectory tracking control for quadrotors with disturbances by using generalized regression neural networks. *Neurocomputing, 460*, 243–255.

Nocedal, J., & Wright, S. J. (2006). *Numerical optimization* (2e ed.). New York: Springer.

Ortiz-Torres, G., Castillo, P., Sorcia-Vázquez, F. D., Rumbo-Morales, J. Y., Brizuela-Mendoza, J. A., De La Cruz-Soto, J., & Martínez-García, M. (2020). Fault estimation and fault tolerant control strategies applied to VTOL aerial vehicles with soft and aggressive actuator faults. *IEEE Access, 8*, 10649–10661.

Pan, T., Fubiao, Z., Jianchuan, Y., & Defu, L. (2021). An integral TSMC-based adaptive fault-tolerant control for quadrotor with external disturbances and parametric uncertainties. *Aerospace Science and Technology, 109*, 106415.

Saeed, A. S., Younes, A. B., Islam, S., Dias, J., Seneviratne, L., & Cai, G. (2015). A review on the platform design, dynamic modeling and control of hybrid UAVs. *International Conference on Unmanned Aircraft Systems (ICUAS), 2015*, 806–815.

Sanz, R., García, P., Zhong, Q.-C., & Albertos, P. (2017). Predictor-based control of a class of time-delay systems and its application to quadrotors. *IEEE Transactions on Industrial Electronics, 64*(1), 459–469.

Shraim, H., Awada, A., & Youness, R. (2018). A survey on quadrotors: Configurations, modeling and identification, control, collision avoidance, fault diagnosis and tolerant control. *IEEE Aerospace and Electronic Systems Magazine, 33*(7), 14–33.

Smeur, E., de Croon, G., & Chu, Q. (2018). Cascaded incremental nonlinear dynamic inversion for MAV disturbance rejection. *Control Engineering Practice, 73*, 79–90.

Song, Y., He, L., Zhang, D., Qian, J., & Fu, J. (2019). Neuroadaptive fault-tolerant control of quadrotor UAVs: A more affordable solution. *IEEE Transactions on Neural Networks and Learning Systems, 30*(7), 1975–1983.

Sun, L., Huo, W., & Jiao, Z. (2017). Adaptive back-stepping control of spacecraft rendezvous and proximity operations with input saturation and full-state constraint. *IEEE Transactions on Industrial Electronics, 64*(1), 480–492.

Tofigh, M. A., Mahjoob, M. J., & Ayati, M. (2018). Dynamic modeling and nonlinear tracking control of a novel modified quadrotor. *International Journal of Robust and Nonlinear Control, 28*(2), 552–567.

Tripathi, A. K., Patel, V. V., & Padhi, R. (2020). Autonomous landing design of UAVs using feedback linearization controller with anti windup scheme. *IFAC-PapersOnLine, 53*(1), 81–86. 6th Conference on Advances in Control and Optimization of Dynamical Systems ACODS 2020.

Wang, Y., Ren, B., Zhong, Q.-C., & Dai, J. (2021). Bounded integral controller with limited control power for nonlinear multiple-input

multiple-output systems. *IEEE Transactions on Control Systems Technology, 29*(3), 1348–1355.
Waslander, S. L., & Wang, C. (2009). Wind disturbance estimation and rejection for quadrotor position control.
Yang, S., Han, J., Xia, L., & Chen, Y.-H. (2020). Adaptive robust servo constraint tracking control for an underactuated quadrotor UAV with mismatched uncertainties. *ISA Transactions, 106*, 12–30.
Zhong, Q.-C., & Rees, D. (2004). Control of uncertain LTI systems based on an uncertainty and disturbance estimator. *Journal of Dynamic Systems, Measurement, and Control-Transactions of the ASME, 126*(4), 905–910.

Julio Betancourt was born in Coahuila, Mexico, on July 20, 1991. He received the B. S. degree in mechatronic engineering from the Universidad Politécnica de Victoria (Mexico) in 2013, the M. Sc. degree in electronic engineering from the Centro Nacional de Investigación y Desarrollo Tecnológico (CENIDET) (Mexico) in 2016, and the Ph.D. degree in automatic control from the University of Technology of Compiègne (France) in 2021. His research topics include modeling and control of unmanned aerial/ground vehicles, robot manipulators, autonomous navigation, real-time embedded control applications and robust disturbance rejection control design.

Pedro Castillo was born in Morelos, Mexico. He received his B.S degree in Electro-mechanic Engineering from the Instituto Tecnológico de Zacatepec, Morelos, Mexico, in 1997, the M. Sc. degree in Electrical Engineering from the Centro de Investigación y de Estudios Avanzados (CINVESTAV), Mexico, in 2000, and the Ph. D. degree in Automatic Control from the University of Technology of Compiègne, France, in 2004. P. Castillo received the best Ph.D. thesis of Automatic Control award from club EEA, (France) in 2005. He has obtained his HDR (Habilitation á Diriger des Recherches) degree from the University of Technology of Compiègne, France in January 16th, 2014. He has held several visiting positions at the University of Sydney, Australia, at the Massachusetts Institute of Technology (MIT), at the Polytechnic University of Valencia, Spain, at Virginia Tech, USA. He has held a detachment position at the LAFMIA UMI CNRS 3175 CINVESTAV -IPN, from December 2012 to November 2014. At the moment, he is researcher (DR) at the French National Research Foundation (CNRS), at the Laboratory Heudiasyc, at the University of Technology of Compiègne, France. His research topics cover : non-linear control, delays systems and predictors, observers, autonomous vehicles, data fusion, robust navigation, real-time control, robotics.

Pedro García received his PhD in Computer Science from the Universitat Politecnica de Valencia, Spain, in 2007, where he is currently an Associate Professor within the Department of Systems Engineering and Automation. He has been a visiting researcher at the Lund Institute of Technology, Lund, Sweden, at the Université de Technologie de Compiègne, France, at the University of Florianopolis, Brazil, at the University of Sheffield, UK, and at the University of Zhejiang, Hangzhou, China. He has coauthored one book, and more than 100 refereed journal and conference papers. His current research interests include control of time-delay systems, disturbance observers and control in type 1 diabetes.

Vicente Balaguer was born in Valencia, Spain, in 1993. He received his BS degree in Industrial Engineering in 2015 and MS in Industrial Engineering, specializing in process control, in 2017, both from the School of Industrial Engineering, Universitat Politecnica de Valencia (UPV), Spain. He is currently working towards his PhD at the same University. He has been a Visiting Researcher at Université de Technologie de Compiègne. His current research interests include control of unstable systems under the effect of disturbances, time-delay systems, and fault-tolerant control.

Rogelio Lozano was born in Monterrey, Mexico, on July 12, 1954. He received the B.S. degree in electronic engineering from the National Polytechnic Institute of Mexico in 1975, the M.S. degree in electrical engineering from Centro de Investigación y de Estudios Avanzados (CINVESTAV), Mexico in 1977, and the Ph.D. degree in automatic control from Laboratoire d'Automatique de Grenoble, France, in 1981. He joined the Department of Electrical Engineering at CINVESTAV, Mexico, in 1981 where he worked until 1989. He was Head of the Section of Automatic Control from June 1985 to August 1987. He has held visiting positions at the University of Newcastle, Australia, from November 1983 to November 1984, NASA Langley Research Center VA, from August 1987 to August 1988, and Laboratoire d'Automatique de Grenoble, France, from February 1989 to July 1990. Since 1990, he

is a CNRS (Centre National de la Recherche Scientifique) Research Director at University of Technology of Compiègne, France. He was Associate Editor of Automatica in the period 1987-2000. He is associate Editor of the Journal of Intelligent and Robotics Systems since 2012. He organized 2 international workshops on UAVs (IFAC RED UAS 2013 and IEEE RAS RED UAS 2015). He was Head of Heudiasyc Laboratory in the period 1995-2007 and since 2008 he is Head of UMI LAFMIA in CINVESTAV. His areas of expertise include UAVs, mini-submarines, exo-squelettons and Automatic Control. He has been the advisor or co-advisor of more than 50 PhD thesis and published more than 200 international journal papers and 10 books.